A bivariate trend analysis to investigate the effect of increasing urbanisation on flood characteristics

[1] Ana I. Requena, [2,3] Ilaria Prosdocimi, [4] Thomas R. Kjeldsen and [1] Luis Mediero

[1] Department of Civil Engineering: Hydraulics, Energy and Environment, Technical University of Madrid, C/ Profesor Aranguren s/n, 28040 Madrid, Spain. (ana.requena@caminos.upm.es; luis.mediero@upm.es).

[2] Centre for Ecology & Hydrology, Maclean Building, Crowmarsh Gifford, Wallingford, OX10 8BB, UK.

[3]Department of Mathematical Sciences, University of Bath, BA2 7AY, (I.Prosdocimi@bath.ac.uk).

[4] Department of Architecture and Civil Engineering, University of Bath, BA2 7AY, Bath, UK (T.R.Kjeldsen@bath.ac.uk).

Corresponding author: Ana I. Requena (ana.requena@caminos.upm.es; Tel.: +34 913365261).

ABSTRACT

Flood frequency analyses are usually based on the assumption of stationarity, which might be unrealistic if changes in climate, land uses or urbanisation impact the study catchment. Moreover, most non-stationarity studies only focus on peak flows, ignoring other flood characteristics. In this study, the potential effect of increasing urbanisation on the bivariate relationship of peak flows and volumes is investigated in a case study in the northwest of England, consisting of an increasingly urbanised catchment and a nearby hydrologically and climatologically similar unchanged rural (control) catchment.

The study is performed via Kendall's tau and copulas. Temporal trends are studied visually and by formal tests, considering variables individually and jointly. Bivariate joint return period curves associated with consecutive time periods are compared to understand the joint implications of such bivariate trends. Although no significant bivariate trends were detected, hydrologically relevant trends were found in the urbanised catchment.

Keywords: copulas, flood trends, Kendall's tau, urbanisation**.**

INTRODUCTION

Accurate design flood estimates with specified return periods are necessary for designing and operating hydraulic structures, such as culverts and dams. Traditionally, flood frequency analyses are based on an assumption of stationarity, i.e., assuming that the flood generating processes remain unchanged over time (e.g., Stedinger *et al*. 1993; Goel *et al*. 1998; Yue *et al*. 1999; Shiau *et al*. 2006). It has long been recognised by hydrologists that stationarity is, at best, a simplified working assumption when changes in urbanisation, land uses or climate are involved in the problem under analysis (e.g., Benkhaled *et al*. 2014), as such impacts can affect the behaviour of hydrological variables, e.g., leading to changes in flood characteristics.

In cases where these effects are considered important, a non-stationarity approach should be applied. Mathematical implementations of non-stationarity into flood frequency models, such as using a non-stationary Generalised Extreme Value (GEV) or Pearson Type 3 (PE3) distributions are relatively straight-forward. However, assessing what is the correct model structure that best describes the impact of changing drivers on the characteristics of the flood series as well as giving realistic predictions of future impacts is far more difficult (Stedinger & Griffis 2011).

The effects of urbanisation on the characteristics of flood runoff have been the subject of several scientific investigations, and it is generally recognised that urbanisation will result in increased runoff volumes (decreased infiltration rates) and reduced catchment lag-times (e.g., Rose & Peters 2001; Shuster *et al*. 2005; Kjeldsen 2009), thus potentially being a significant cause of non-stationarity in flood series impacting both peak flow values and runoff volumes (e.g., Sheng & Wilson 2009).

Much attention has been given to studying trends in peak flow values as a function of time (Petrow & Merz 2009; Wilson *et al*. 2010; Mediero *et al*. 2014), with some exceptions such as the approach presented by Bender *et al*. (2014) for analysing bivariate non-stationary in an uncommonly long peak-volume flood data record (191 years). Indeed, as it is expected that increased urbanisation will lead to changes in other flood characteristics other than the peak flow, in particular the flood volume, a study of the potential changes in multiple variables is necessary to better understand the changes that could affect flood risk under increasing urbanisation. The present study aims to introduce and discuss a simple and general framework to investigate changes of multivariate flood characteristics under increasing urbanisation. This is performed by studying the univariate and bivariate properties of peak (Q) and volume (V) in two paired case catchments located in the northwest of England. Changes in the univariate peak flow values for these two catchments have already been assessed in Prosdocimi *et al.* (2015), who found that the increase of urbanisation in Catchment 70005 was connected to increasing trends, especially for summer flows. The present work wishes to complement such a study by proving the conceptual framework needed to investigate the bivariate behaviour of flow peaks and flood volume. The analysis of this case study is especially relevant due to the available information about urbanisation levels and flow records of high quality, something not easily found. Nevertheless, the available

hydrological record is relatively short and the results presented in this work should be considered as preliminary and taken with caution. The two catchments are hydrologically and climatologically similar, except for the increasing urbanisation levels which affect one of them but not the other. The differences in the changes in the flood characteristics in the two catchments can be imputed to the changes in the land cover of the urbanised catchment. Changes in the association of the bivariate distribution of (*Q*,*V*) are investigated by both the Kendall's tau (τ), a rank-based dependence measure, and copulas for bivariate design flood analysis. Copulas (e.g., Joe 1997), which have found several applications in multivariate hydrological analysis (e.g., De Michele *et al*. 2005; Renard & Lang 2007; Klein *et al*. 2010; Ganguli & Reddy 2013; Requena *et al*. 2015), allow obtaining the multivariate joint distribution of multiple random variables by characterising the relation of dependence among them, incorporating the corresponding univariate marginal distributions that can belong to different families.

CASE STUDY AND DATA EXTRACTION

The two catchments of this study are located in the northwest of England (Figure 1). High-quality runoff time series of 15min resolution recorded by the Environment Agency are available for the common period 1976–2008. The urbanised catchment is drained by the River Lostock and flow data are recorded at Littlewood Bridge (gauging station numbered 70005). In this catchment there has been a relatively high degree of rural land-use being transformed into build-up areas (urbanisation) over the past 40 years; from 9% in 1976 to 16% in 2008 as shown in Figure 2. The temporal change in catchment urban extent was computed at decadal time steps using the methodology presented by Miller & Grebby (2014) from historical 1:10 000 topographic maps.

The rural catchment drained by the River Conder is a nearby hydrologically and climatologically similar catchment, where flow data is recorded near Galgate (gauging station numbered 72014). This is a predominantly rural catchment, which has experienced little change in the study period. Hereafter the catchments are referred to with their gauging station number: the urbanised catchment corresponds to Catchment 70005, and the rural one to Catchment 72014.

Table 1 displays key catchment descriptors from Institute of Hydrology (1999) for the catchments under study: catchment area (AREA), baseflow index as predicted by the Hydrology of Soil Type (BFIHOST), Standard-period (1961-1990) Average Annual Rainfall (SAAR), flood attenuation from upstream lakes and reservoirs (FARL), and proportion of the catchment covered by the 100-year floodplain (FPEXT). The two catchments are deemed hydrologically similar according to the similarity measure developed in Kjeldsen & Jones (2009). The finding of a suitable paired catchment should be based on similarities in both hydrological and climatological terms. The importance of identifying a catchment with a similar climatology is a key step for a robust attribution of flood trends to increasing urbanisation (Shastri *et al*. 2015), and the catchments used in this study were the best match given the paucity of long, high quality flow records. In the present study, catchments have similar geographical conditions, being nearby and entailing a similar gauging station elevation. Besides, flood events are of the synoptic type for both catchments (Mediero *et al*. 2015). They also entail a similar annual precipitation (SAAR in Table 1), as well as similar oscillations for different quantiles of the catchment average daily rainfall series (Figure 3). Hence, a similar climate is considered.

The water year in the UK runs from October to September: events occurring between October and March (included) are classified as winter events, while the period April to

September constitutes the summer months. The water year 1988–1989 was removed from the study period, as no summer events were available for the gauging station 72014 in this year.

The period 1976–2008 was divided into two equally sized time windows (e.g., Shastri *et al.* 2015), representative of periods of low and high urbanisation levels for Catchment 70005, respectively. Note that by using two equally sized time periods the uncertainty in the estimates for the two time windows can be assumed to be of a similar scale. Only two time windows were considered because of the relatively short common data, although if longer data records were available, the procedure could be applied considering a greater number of time windows. The first time window (named as W1) runs from 1976 to 1992; while the second period (W2) runs from 1993 to 2008. Therefore, the data series (Q_m, V_m) (ordered in time), with $m = 1 : n_{tot}$ and n_{tot} the total number of water years, is also divided into (Q_k^{W1}, V_k^{W1}) and (Q_k^{W2}, V_k^{W2}), with $k = 1 : n_{tot}/2$. Here (Q_k^{W1}, V_k^{W1}) represent the first $n_{tot}/2$ pairs of (Q_m, V_m) and (Q_k^{W2}, V_k^{W2}) the last $n_{tot}/2$ pairs. To simplify formulas, hereafter the pairs are presented as (Q_i, V_i) with $i = 1 : n$. Depending on the time period considered, (Q_i, V_i) makes reference to (Q_m, V_m), (Q_k^{W1}, V_k^{W1}) or (Q_k^{W2}, V_k^{W2}), with *n* the corresponding data length in each case.

A simple method for extracting the bivariate properties of flood events is considered to study the effect of urbanisation on the typical shape of hydrographs, as it is characterised by the strength of the correlation between peak flow and a measure of flood volume. Traditional techniques for baseflow separation work with daily data (Chapman 1999; Eckhardt 2008). However, this method should be applicable in an empirical data-based study; and it should work with highly variable sub-hourly data,

145 rather than more smooth daily data. Then, because of the difficulty of isolating
146 individual flood hydrographs generated by distinct rainfall events, and due to the focus
147 of this study is to analyse the joint properties of volume and flood peak, the measure of
148 flood volume, *V*, adopted in this study is defined as the part of the event hydrograph
149 above a threshold set at 40% of the flood peak *Q*, i.e., V is considered as the volume
150 associated with the upper 60% of the flood event. By considering only flow above a
151 relatively high threshold, the event volumes were not unduly influenced by post-peak
152 small amounts of rainfall causing the flow to increase part way down the recession
153 curve. The 40% threshold used in this study was found to be sufficiently high to remove
154 the nuisance effects caused by secondary rainfall inputs while maintaining the
155 generality of the results. Also note that volumes extracted using different thresholds
156 were found to be correlated. In this regard, for instance, Karmakar & Simonovic (2007)
157 reported a highly significant correlation between peak and volume regardless of the
158 discharge threshold level. Note that a more detailed analysis of each individual event
159 would not result in more informative results, but rather lead to a less transparent
160 analysis. As an example, the identification of the (Q_i, V_i) pair associated with a given
161 water year *i* is shown in Figure 4.

162 For both catchments, the annual, summer and winter maxima of the instantaneous peak
163 flow value are identified and the corresponding volumes are extracted. Seasonal
164 maxima are also investigated to better understand whether the changes seen in the
165 annual series are driven by changes in a specific type of events. The autocorrelation for
166 the annual and seasonal series has been plotted and tested, indicating that the standard
167 iid assumption is verified (not shown). Types of floods were not analysed because
168 floods in UK mainly belong to the synoptic type (Mediero *et al*. 2015). In summary two
169 catchments are studied, 70005 (urban) and 72014 (rural), two event characteristics are

considered (*Q* and *V*), three maximum series of events are extracted (winter, summer and annual maximum flow events), and three time periods are considered: 1976–1992 (W1), 1993–2008 (W2) and 1976–2008 (whole series).

METHODOLOGY AND RESULTS

The investigation of potential changes in the *Q*-*V* relationship proceeds as follows: at first trends in the univariate series for *Q* and *V* separately and in the association between the two variables are studied. Then, a non-parametric procedure is used to assess the statistical significance of the observed trends. Finally, changes in the bivariate return period curves computed via copulas are investigated. Results for the two catchments under study are shown directly after the description of the methodological steps.

Analysis of univariate flood trends in *Q* and *V* series

The first step of the methodology consists in the analysis of univariate temporal trends in the flood series, using visual inspection and the widely used Mann-Kendall test (e.g., Villarini *et al*. 2009; Coch & Mediero 2015), a non-parametric test based on Kendall's τ. The Mann-Kendall test (Kendall 1975) is used to assess the null hypothesis of no association between two variables, and the presence of significant temporal trends can be assessed by taking time as one of the variables. The statistical significance is assessed with a two-sided test at a 95% confidence level.

Figure 5 shows the evolution in time of the *Q* and *V* annual and seasonal series for Catchment 70005 and Catchment 72014 (see Table 1 for descriptive statistics). A smaller variation in time of *Q* and *V* can be seen in Catchment 70005 in comparison to the characteristics of the flood events recorded in Catchment 72014. To ease the visual identification of trends least squares fits are superimposed to each plot. Overall, the regression slopes for *Q* appear to be steeper than those for *V*. Indeed, *p*-value of the

Mann-Kendall test indicate that only the trends of the annual and summer peak flow series in Catchment 70005 are statistically significant at a 5% significance level (Table 2).

Analysis of bivariate flood trends via Kendall's τ

Bivariate trends are assessed through an exploratory analysis of the relationship between *Q* and *V* using both graphical tools and a non-parametric measure on changes in the dependence between the variables, as estimated by the Kendall's τ. Finally, hydrograph shape and its connection with Kendall's τ is also analysed. Note that the whole methodology followed in this section is first presented and later results are displayed.

First a scatter plot of the $(R_i/(n+1), S_i/(n+1))$ pairs, where R_i is the rank of Q_i and S_i is the rank of V_i (with $i = 1,\ldots,n$) is drawn for winter, summer and annual maximum flow events for both catchments under study. These plots provide a visual assessment of the dependence between variables. Note that scatter plots are linked to the Kendall's τ value, as the latter is a rank-based measure: more scattered ranks lead to smaller Kendall's τ values (i.e., lower association), whereas less scattered ranks will entail the opposite.

Next, changes in hydrograph shapes over time are investigated. The standardised mean flood hydrographs of the *Q*-*V* pairs for a given time window (whole series, W1 or W2) are plotted together by locating their time of peak on the same vertical (Miller *et al.* 2014), with the aim of visually comparing their average shape. Note that the mean flood hydrographs are standardised by the largest observed peak value (Q_{peak}) in the sample, considering the entire data length. The corresponding point-wise confidence intervals

217 ($\bar{y}-s, \bar{y}+s$) are also obtained, where $\bar{y}$ and s are the mean and standard deviation,
218 respectively, of the standardised flow values at each time step. This analysis is carried
219 out considering winter, summer and annual flood hydrographs.

220 The link between the hydrograph shape (which depends on the values of *Q* and *V*) and
221 Kendall's τ, can be understood by studying the relation between the corresponding
222 hydrograph shapes and the $(R_i/(n+1), S_i/(n+1))$ pairs. A didactic example extracted
223 from the annual data in Catchment 72014 is shown in Figure 6, in which specific a_l
224 pairs with $l = 1:7$ are selected from the scatter plot (Figure 6a). Overall, three distinct
225 clusters of events are evident. The first set is composed of pairs positioned close to the
226 main diagonal (e.g., a_1, a_2 and a_3). The second set consists of pairs located below the
227 main diagonal (e.g., a_4 and a_5). Finally, pairs located above the main diagonal (e.g.,
228 a_6 and a_7) constitute the third set. Each set is associated with a particular standardised
229 hydrograph shape, as it can be seen in Figure 6b generated following the procedure
230 explained in the previous paragraph. Shapes related to points in the second set are
231 steeper than the pairs of the first set. The opposite applies to the points of the third set,
232 where shapes are less flashy. Therefore, the closer the pairs are to the main diagonal
233 (i.e., the larger is Kendall's τ, as the larger is the correlation), the more balanced and
234 similar are the shape of the events. On the other hand, points located far away from the
235 diagonal, which would lead to smaller values of Kendall's τ, are generally characterised
236 by a larger variability in the hydrograph shapes.

237 The relationship between *Q* and *V* in the case study is investigated in Figure 7. The
238 scatter plots show the interplay of the scaled ranks of the two univariate variables, and
239 they are generated by first using the complete record, followed by a plot considering
240 each of the two time windows W1 and W2 (Figure 7a). Overall, it was found that ranks

241 related to W1 are more scattered than to W2 for Catchment 70005. The value of
242 Kendall's τ is also derived for each time window and drawn in a new plot to facilitate
243 the visual identification of the possible trend (Figure 7b). 95% confidence intervals are
244 also displayed in Figure 7b (Schneider *et al*. 2015). The Kendall's τ value is smaller for
245 W1 (indicating a more weak correlation) than for W2 (indicating a stronger correlation)
246 in Catchment 70005, as expected from the results of the scatter plots. Therefore, an
247 increase over time was observed in Kendall's τ for Catchment 70005. The opposite was
248 found for Catchment 72014.

249 The increasing correlation levels found in Catchment 70005 suggest that the hydrograph
250 shapes for this catchment would tend to become more regular in time, according to what
251 observed in Figure 6. On the contrary, the decrease of correlation seen in Catchment
252 72014 would indicate a larger variability of the flood hydrograph for this catchment. A
253 comparison between hydrograph shapes from the two time windows is shown in Figure
254 8. The mean and confidence intervals of the hydrograph shape associated with the entire
255 data record are also shown for illustration purposes. As it can be seen, the value of the
256 peak of the mean hydrograph increases from the first time period W1 to the second
257 period W2 for winter, summer and annual events (for both catchments). Note that the
258 largest increase is found for summer maximum flow events of Catchment 70005.
259 Results regarding confidence intervals support the Kendall's τ analysis presented in the
260 previous paragraph, showing that the difference between confidence interval boundaries
261 decreases from W1 to W2 for Catchment 70005 (i.e., the difference between events
262 decreases), while the opposite holds for Catchment 72014 (Figure 8) . No noticeable
263 differences were identified between mean hydrograph shapes, in neither of the time
264 windows nor catchments.

265 **Trend significance assessment: a permutation procedure**

A permutation test is suggested to check if the peak flow Q, the volume V or the Kendall's τ coefficient are statistically different in the two time windows W1 and W2. This is slightly different from testing whether time is related to the variable of interest, as in the Mann-Kendall test, and allows using the same procedure to assess both univariate and bivariate temporal flood trends. Also, permutation tests are non-parametric (as well as the Mann-Kendall test) so that no formal distributional assumption for the data is needed in order for the test to be valid, and, in some situations, they provide exact inference (see, e.g., Ernst 2004; Good 2005, for an introduction on permutation methods). The testing procedure consists of the following steps: (i) choose a test statistic which gives a good representation of the scientific question at hand; (ii) compute the test statistic for the observed data t_{obs}; (iii) permute without replacement the observed sample for $N_{\text{perm}} = 10\,000$ times; (iv) for each permuted sample compute the test statistic $t_{\text{perm,i}}$, with $i = 1 : N_{\text{perm}}$; (v) estimate the empirical distribution (F_n) of the test statistic using all the N_{perm} permuted samples and compute the (two-tailed) p-value as:

$$p - value = 2\min\left(\frac{\sum_{i=1}^{N_{\text{perm}}} 1_i}{N_{\text{perm}}+1}, \frac{\sum_{i=1}^{N_{\text{perm}}} (1-1_i)}{N_{\text{perm}}+1}\right), \quad \text{where } 1_i = \begin{cases} 1 & t_{\text{perm}}(i) > t_{\text{obs}} \\ 0 & t_{\text{perm}}(i) \le t_{\text{obs}} \end{cases} \tag{1}$$

For p-values greater than 0.05 the null hypothesis is accepted at a 95% confidence level.

In this study, permutation methods are used to test if the location of the distribution of both Q and V in the two different time windows is different. The difference between the sample median (m_Q and m_V) in the two time windows is chosen as the test statistic to represent the null hypothesis of equal locations. The observed difference between the sample medians is compared with the distribution of the difference in the medians for

288 the permuted samples and the associated *p*-value is computed as in Equation (1).
289 Similarly, to further support the visual evidence of the previous sub-section, the null
290 hypothesis of constant association between Q and V is tested by using the difference
291 between Kendall's τ in the two windows as a test statistic.

292 *P*-values from Equation (1) by applying the permutation procedure to the case study are
293 shown in Table 3. Among the positive observed differences between m_Q and m_V in W1
294 and W2 for both catchments considering winter, summer and annual maximum flow
295 events, only the difference associated with summer maximum flow events of Catchment
296 70005 can be considered significant. Note that this trend was also found to be
297 significant when the Mann-Kendall test was applied considering the whole data length
298 (first sub-section of Methodology and Results Section). For the Kendall's τ, neither the
299 increase for Catchment 70005 nor the decrease for Catchment 72014 were found to be
300 statistically significant for any season.

301 **Analysis of bivariate flood trends by comparison of return period curves**

302 In the bivariate (Q-V) space, an infinite set of events given by their Q-V pairs are
303 located under the same return period curve, which can be estimated by copulas
304 (Salvadori & De Michele 2004; Requena *et al*. 2013). In this regard, the final step of the
305 assessment of the impact of urbanisation on flood properties entails the analysis of
306 trends in the bivariate Q-V space by the comparison between the return period curves in
307 windows W1 and W2, for a set of given return period values. As an initial step, the
308 analysis involves the selection of the joint distribution of (Q,V) that best characterises
309 the statistical behaviour of the variables, composed of the marginal distributions of Q
310 and V and a copula.

311 Although the information gained by studying the seasonal series can be useful for
312 identifying potential changes in the flood seasonality, the analysis of the bivariate return
313 period curves will focus on the annual series, since these are the ones that would be
314 used to estimate design floods. The methods could also be applied to summer or winter
315 maximum flow series.

316 **Selection of a joint distribution: margins and copula**

317 Following Sklar's theorem (Sklar 1959), the joint cumulative distribution function of
318 the random variables *Q* and *V*, $H(q,v)$, can be expressed as:

319 $$H(q,v) = C(F_Q(q), F_V(v)), \quad q,v \in \Re, \tag{2}$$

320 where *q* and *v* are given values of the variables *Q* and *V*, $F_Q(\cdot)$ and $F_V(\cdot)$ are the
321 marginal cumulative distributions functions of *Q* and *V*, respectively; and *C* is the
322 copula function, i.e., a joint cumulative distribution function with uniform margins.
323 Thus Equation (2) can be expressed as $C(u_1,u_2)$, where $u_1 = F_Q(q)$ and $u_2 = F_V(v)$.
324 The selection of both the marginal distributions that best represent the individual
325 variables, and the copula function that best characterises the dependence between *Q* and
326 *V* is then needed to achieve a complete description of $H(q,v)$.

327 Several distributions used in hydrology, such as the GEV, Generalised Logistic (GLO),
328 Generalised Normal (GNO), Generalised Pareto (GPA) and PE3 were considered as
329 potential marginal distributions of *Q* and *V*. The distribution that best characterises the
330 observed data was selected using the L-moment ratio diagram, in which the relations
331 between the theoretical coefficients of L-skewness (τ_3) and L-kurtosis (τ_4) for different
332 three-parameter distributions are shown through curves (Hosking & Wallis 1997). The
333 sample estimates of the coefficients of L-skewness (t_3) and L-kurtosis (t_4) are also

plotted in the same diagram, choosing the distribution curve closest to the sample values. The choice of the marginal distribution for each variable was performed using the series covering the whole data length, and the selected distribution applied to both time periods. This larger sample ensures that estimates of t_3 and t_4 are less biased. Location (ξ), scale (σ) and shape (γ) parameters of the three-parameter marginal distributions ($F_Q(\cdot)$ and $F_V(\cdot)$) are estimated by the method of L-moments. Since estimates of the shape parameter have a high uncertainty when using a short record (Stedinger & Lu 1995), the estimate $\hat{\gamma}$ obtained using the complete data series was used in each of the two time windows to reduce the uncertainty originating from the third-order statistic estimates.

In order to identify the copula that best characterises the dependence structure between *Q* and *V*, a representative set of potential copulas was tested: the Clayton, Frank and Gumbel copula belonging to the Archimedean family; the Galambos (and also the Gumbel) copula belonging to the extreme-value family and the Plackett copula representing other families. The goodness-of-fit test used for identifying possible copula candidates (see Genest *et al*. 2009) is based on the Cramér-von Mises statistic (S_n):

$$S_n = \sum_{i=1}^{n} \left\{ C_n\left(\frac{R_i}{n+1}, \frac{S_i}{n+1}\right) - C\left(\frac{R_i}{n+1}, \frac{S_i}{n+1}; \hat{\theta}\right) \right\}^2 , \quad (3)$$

where $C_n(.)$ is the empirical copula and $C(\cdot)$ is the estimated copula with a $\hat{\theta}$ parameter (obtained by the inversion of Kendall's τ method). The *p*-value needed to formally test if the copula is suitable is estimated by a validated bootstrap procedure (Genest & Rémillard 2008). This procedure (in a similar way to the aforementioned permutation procedure) derives an empirical distribution of the test statistic, S_n, using 10 000 simulations. The copula is acceptable if the *p*-value is greater than 0.05.

Additional information is needed to choose the best copula among the ones that have passed the goodness-of-fit test. By assessing the upper tail dependence, a further analysis to check the ability of each copula to characterise the extreme values of the studied variables is carried out (e.g., Poulin *et al*. 2007). For this purpose, the non-parametric upper tail dependence coefficient of the observed data, $\hat{\lambda}_U^{CFG}$, is compared with the theoretical upper tail dependence coefficient, $\hat{\lambda}_U$, of each copula (formulas in Frahm *et al*. 2005). The copula is considered more appropriate as smaller is the difference between $\hat{\lambda}_U^{CFG}$ and $\hat{\lambda}_U$ values. Remark that however, the reliability of $\hat{\lambda}_U^{CFG}$ is limited, especially for a short data length. Moreover, the use of the Akaike information criterion (AIC) as model selection criterion (Akaike 1974) can be helpful for ranking the candidate copulas. Based on the latter, the best copula would be that with the smallest AIC value.

Although in the present case study the observed changes in time considering jointly Q and V (i.e., Kendall's τ trends in Trend Significance Assessment Sub-section) were not identified as statistically significant (with p-values equal to 0.132 and 0.465 for Catchment 70005 and 72014, respectively, see Table 3), they could still be hydrologically relevant. Therefore, the implications of such trends for the flood hydrograph shape should be analysed. For this analysis, the bivariate joint distribution of the observed data was estimated for both time windows.

The marginal distribution $F_Q(\cdot)$ was chosen to be a GLO, which is generally the preferred distribution for annual maximum peak flow data in the UK (Institute of Hydrology 1999). However, no guidance exists in reference to hydrograph volumes, V. The sample L-moment ratios of the V series for each catchment were plotted on an L-moment ratio diagram (Figure 9). Figure 9 also shows the 95% confidence ellipsoids

based on the bivariate distribution of L-skewness and L-kurtosis, which are the basis of the goodness-of-fit measure introduced by Kjeldsen & Prosdocimi (2015). The thicker lines indicate the distributions that can be accepted according to the goodness-of-fit measure; the selected distribution corresponds to the one for which the measure is minimised for each catchment. The GLO distribution was selected to represent *V* for Catchment 70005, while the GEV distribution was chosen for Catchment 72014. The estimated parameters of the marginal distributions are shown in Table 4. As it can be seen, the urban catchment has larger location parameters than the rural catchment, while for both catchments and variables the skewness is negative. The estimated fitted marginal flood frequency curves are displayed in Figure 10 along with the observed data series. In the case of Catchment 70005, the marginal curve corresponding to W1 intersects that corresponding to W2 for both *Q* and *V*. That is, if small univariate return periods (*T*) are considered, larger values of *Q* and *V* are expected for W2; the contrary happens for larger *T* values. Intersection between marginal curves is not observed in Catchment 72014.

Results for the copula selection criteria are shown in Table 5. Most of the considered copulas passed the goodness-of-fit (i.e., *p*-values greater than 0.05), with the exception of the Clayton copula that is rejected for several cases. Since all cases present upper tail dependence, i.e., $\hat{\lambda}_U^{CFG}$ is greater than zero, the previously accepted copulas are cut down accordingly to the $\hat{\lambda}_U$ values. In this regard, the Gumbel and Galambos copulas show $\hat{\lambda}_U$ values close to $\hat{\lambda}_U^{CFG}$. Consequently, both of them could be chosen, as the results of the AIC are also very similar. Because of the results in Table 5 and its properties, the Gumbel copula was selected for the three time periods and both catchments. This copula was also selected as the best copula in characterising the

405 dependence between peak flow and volume in other studies (e.g., Zhang & Singh 2006;
406 Poulin *et al*. 2007; Karmakar & Simonovic 2009; Requena *et al*. 2013; Sraj *et al*. 2015).

407 **Comparison between bivariate joint return period curves**

408 Bivariate joint return period curves are used here to investigate changes in flood events
409 between W1 and W2. Combination of values belonging to the return period curves can
410 be estimated by the selected copula. In this study, the bivariate return period used for
411 analysing changes in flood events is the widely used OR return period (T_{OR}) (Salvadori
412 & De Michele 2004), in which the thresholds *q* or *v* are exceeded by the random
413 variable *Q* 'or' *V*, respectively (Equation (4)).

414 $$T_{\mathrm{OR}} = \frac{\mu_T}{P(Q > q \vee V > v)} = \frac{\mu_T}{1 - P(Q \le q \wedge V \le v)} = \frac{\mu_T}{1 - C(F_Q(q), F_V(v))} = \frac{\mu_T}{1 - C(u_1, u_2)}, \quad (4)$$

415 where μ_T is the mean inter-arrival time between two successive events, with $\mu_T = 1$ for
416 annual maximum series. Finally, return period curves are obtained in original units by
417 transforming the (u_1, u_2) pairs with the same T_{OR} into $(Q_{sim}, V_{\mathrm{sim}})$ pairs by Equation (5),
418 using the previously selected marginal distributions.

419 $$Q_{\mathrm{sim}} = \hat{F}_Q^{-1}(u_1), \quad V_{\mathrm{sim}} = \hat{F}_V^{-1}(u_2), \quad (5)$$

420 where $\hat{F}_Q^{-1}(\cdot)$ is the inverse marginal distribution of *Q*, $\hat{F}_Q(\cdot)$. The same holds for
421 $\hat{F}_V^{-1}(\cdot)$. The bivariate return period curves associated with the separate time windows
422 W1 and W2 and the whole data length are calculated.

423 Probability level curves (of the copula) for several values of *p* (i.e., points fulfilling
424 $C(u_1, u_2; \hat{\theta}) = p$, where *p* is the simultaneous non-exceedance probability of the two
425 variables) for both study catchments are shown in Figure 11. The plot also shows 100
426 000 (u_1, u_2) pairs randomly generated from the fitted copula (grey points), showing that

smaller Kendall's τ values lead to a more scattered data. Results for W1, W2 and the entire record are plotted and compared for both catchments. In Catchment 70005, curves related to W2 (with larger Kendall's τ) are located below those corresponding to W1 (with smaller Kendall's τ), while converging in the extremes (i.e., the asymptotes). The opposite occurs for Catchment 72014. As expected, curves related to the whole data length are located between W1 and W2 curves.

Figure 12 shows simulated copula values and bivariate joint return period curves associated with $T_{\mathrm{OR}} = 2, 5, 100$ and 250 years (Equation (4)) in original units (by Equation (5)). It should be noted that the results for high return periods should be taken with caution, due to the relatively short data length available and the consequent large uncertainty; yet they are shown as illustration. For Catchment 70005, curves move downward to the left (from W1 to W2) as larger is the return period. Overall, the decrease is larger for *Q* than for *V*, reflecting the findings for the univariate distributions (Figure 10). This means that flood events tend to have a lower peak value, while at the same time the flood hydrographs tend to be less flashy. For instance, the vertex of the 100-year return period curve for the urban catchment undergoes a 9.4% decrease in peak and a 7.6% decrease in volume from W1 to W2. Also, in accordance with the results presented in Figure 10, such a trend differs for small return periods, as margins of different time windows cross at $T_{\mathrm{OR}} \cong 5$ for *Q* values, while at $T_{\mathrm{OR}} \cong 2-5$ for *V* values. However, the opposite is observed for Catchment 72014, as return period curves move upward to the right. Such a shift is larger for *Q*, meaning that flood events would become larger, while flood hydrographs steeper. This is also in accordance with the results obtained in the univariate case (Figure 10), where the increase of *Q* is greater than that of *V*. For instance, the vertex of the 100-year return period curve for the rural catchment undergoes a 20.3% increase in peak and a 14.1% increase in volume from

W1 to W2. Note that for both catchments, a higher return period generally results in a larger shift of the curve. This could be caused by the increasing uncertainty related to increasing return periods, in particular with the small sample sizes available in this study.

In case that an estimate of a design flood is required, the effect of changes in urbanisation extent on return period curves can be assessed using the results associated with W2. Alternatively, if stationarity is assumed the most reliable estimate will be obtained by using the return period curves associated with the whole data length. Also, differences between return period curves in the two time windows (of Catchment 70005) give some insight into how the curves move in time because of the urban development. Consequently, this behaviour could be extrapolated in the future by using predictions of the urbanisation increase level expected in a given catchment.

DISCUSSION

Significant univariate trends in the observed peak value *Q* for summer maximum flow events in the urban catchment (70005) have been identified by both the Mann-Kendall test and the permutation procedure. The Mann-Kendall test also found a significant trend in the observed annual maximum flow events in this catchment. No significant univariate trends were found, neither in the observed volume *V* nor in any of the variables extracted from the rural catchment (72014). The results of trends in the seasonal series help understanding from which types of events the trends in the annual series are most likely to be driven. The results suggest that for the urbanised catchment the potential changes in the annual series would mostly be driven by change for the summer events.

The visual analysis of bivariate (Q,V) series found an increase in Kendall's τ over time for Catchment 70005, leading to increasingly more regular hydrograph shapes; whereas the opposite was found for Catchment 72014, resulting in a larger variability of flood hydrograph shapes. The visual analysis of the hydrograph shape variability in time, using confidence intervals, confirmed this result.

The analysis of bivariate trends in the characteristics of flood events in the urban catchment found no statistically significant trends based on Kendall's τ. However, opposite results to those found in the rural catchment were obtained. The implications of such trends when considering bivariate return period curves were also opposite, suggesting that the trend in the urban catchment may be caused by changes in the flood generating processes that may not be statistically detected. Thus, it is likely that, if indeed a change is occurring in some of the flood characteristics, a larger sample size would be needed for standard statistical tests to detect it (see also Prosdocimi *et al*. 2014, for a discussion on sample size problems in the analysis of hydrological series). The selection and fit of both margins and copula would be more powerful and accurate if longer data series were available; and large uncertainties in the estimate of both margins and copula could have affected the results.

In addition, two larger flood events observed in the first time-window (W1) in Catchment 70005 could lead to larger quantiles for high return periods than in the case of W2. Therefore, as W1 and W2 are short, both univariate and bivariate estimates for high return periods are highly dependent on the magnitude of the observed flood events and, consequently, on the magnitude of rainfall events that drove such flood events in each period. Finally, it is also interesting to highlight that the effect of the bivariate trend found (for high return periods) in the urban catchment is different from what would normally be expected in an urbanised catchment, as in general urbanisation

should lead to steeper hydrograph shapes. A possible explanation could also be the influence of the sewer system or local flood mitigation measures when high return period floods are considered, although looking into the causes is beyond the scope of this paper. Also, results may point towards a more complex interaction between urbanisation and flood characteristics than commonly assumed.

Remark that in future studies, the results of the present preliminary analysis could be compared with those obtained by applying the proposed methodology to a much longer data length (when it is available), as well as to flood events identified by applying a detailed hydrograph separation method, for which an exhaustive analysis of rainfall and streamflow should be performed.

CONCLUSIONS

A simple and general framework to investigate the effect of changes in a catchment land cover on the univariate and bivariate behaviour of some flood characteristics is introduced. The case study is composed of two nearby hydrologically and climatologically similar catchments in the northwest of England, where the most important difference is the increasing urbanisation extent in the urban catchment; hence any difference observed in time can mostly be attributed to urbanisation. In general, no statistical evidence of temporal change was identified in the univariate series, apart from an increasing trend in summer peak flows in the urban catchment. It should be mentioned that the permutation test used for trend significance assessment on the differences between the location of the distribution of a given variable might be applicable to other hydrological analyses.

The potential bivariate trend due to increasing urbanisation in the urban catchment was found to lead to smaller flood peaks and less flashy flood hydrographs. However, these

results could be conditioned to the short available records and the use of larger data sets could be advisable for its confirmation. In addition, further research in the identification and modelling of the process control on storm runoff in urban catchments could help in understanding this finding.

The methodology presented in this work could be applied to any pair of catchments that can be considered hydrologically and climatologically similar except for one major characteristic, which has changed in one of the two catchments. Finally, the proposed methodology can help practitioners to describe trends in flood characteristics, in order to improve estimates of the design floods by a non-stationarity approach.

ACKNOWLEDGEMENTS

This work has been supported by the COST Office grant ES0901 *European procedures for flood frequency estimation* (FloodFreq), via the Short Term Scientific Mission (STSM) program. The authors are also grateful for the financial contribution made by the *Carlos González Cruz* Foundation and the project 'MODEX-Physically-based modelling of extreme hydrologic response under a probabilistic approach. Application to Dam Safety Analysis' (CGL2011-22868), funded by the Spanish Ministry of Science and Innovation (now the Ministry of Economy and Competitiveness). The authors thank James Miller for the urbanisation extent data shown in Figure 2.

REFERENCES

Akaike, H. 1974 A new look at the statistical model identification. IEEE Transactions on Automatic Control. **19**(6), 716–723.

Bender, J., Wahl, T. & Jensen, J. 2014 Multivariate design in the presence of non-stationarity. *J. Hydrol*. **514**, 123–130.

547 Benkhaled, A., Higgins, H., Chebana, F. & Necir, A. 2014 Frequency analysis of annual
548 maximum suspended sediment concentrations in Abiod wadi, Biskra (Algeria).
549 *Hydrol. Process.* **28**(12), 3841–3854.

550 Chapman, T. 1999 A comparison of algorithms for stream flow recession and baseflow
551 separation. *Hydrol. Process*. **13**, 701–714.

552 Coch, A. & Mediero, L. 2015 Trends in low flows in Spain in the period 1949–2009.
553 *Hydrolog. Sci. J.* DOI**:**10.1080/02626667.2015.1081202

554 De Michele, C., Salvadori, G., Canossi, M., Petaccia, A. & Rosso, R. 2005. Bivariate
555 statistical approach to check adequacy of dam spillway. *J. Hydrol. Eng.* **10**, 50-57.

556 Eckhardt, K. 2008 A comparison of baseflow indices, which were calculated with seven
557 different baseflow separation methods. *Journal of Hydrology*. **352**(1-2), 168-173.

558 Ernst, M. D. 2004 Permutation methods: a basis for exact inference. *Stat. Sci*. **19**, 676–
559 685.

560 Frahm, G., Junker, M. & Schmidt, R. 2005 Estimating the tail-dependence coefficient:
561 properties and pitfalls. *Insur. Math. Econ*. **37**, 80–100.

562 Ganguli, P., & Reddy, M. J. 2013 Probabilistic assessment of flood risks using trivariate
563 copulas. *Theor. Appl. Climatol*. **111**(1–2), 341–360.

564 Genest, C. & Rémillard, B. 2008 Validity of the parametric bootstrap for goodness-of-
565 fit testing in semiparametric models. A*nnales de L'Institut Henri Poincaré-*
566 *Probabilités Et Statistiques*. **44**(6), 1096–1127.

567 Genest, C., Rémillard, B. & Beaudoin, D. 2009 Goodness-of-fit tests for copulas: a
568 review and a power study. *Insur. Math. Econ*. **44**(2), 199–213.

569 Goel, N., Seth, S. & Chandra, S. 1998 Multivariate modeling of flood flows. *J. Hydraul.*
570 *Eng-Asce*. **124**(2), 146–155.

571 Good, P. 2005 *Permutation, parametric and bootstrap tests of hypotheses*. Springer
572 Series in Statistics, New York, 315 pages.

573 Hosking, J.R.M, & Wallis, J.R. 1997 *Regional frequency analysis: an approach based*
574 *on L-moments*. Cambridge University Press, Cambridge, 224 pages.

575 Institute of Hydrology. 1999 *Flood Estimation Handbook*, Vol. 5. Institute of
576 Hydrology, Wallingford, UK.

577 Joe, H. 1997 *Multivariate model and Multivariate dependence concepts*. Chapman and
578 Hall/CRC Monographics on Statistics and Applied Probability, London, 424 pages.

579 Karmakar, S. & Simonovic S. P. 2009 Bivariate flood frequency analysis. Part 2: a
580 copula-based approach with mixed marginal distributions. *Journal of Flood Risk*
581 *Management*. **2**, 32–44.

582 Karmakar, S. & Simonovic. S. P. 2007 Flood frequency analysis using copula with
583 mixed marginal distributions. Water resources research report.

584 Kendall, M. G. 1975 Multivariate analysis. London, Griffin.

585 Kjeldsen, T. R. 2009 Modelling the impact of urbanisation on flood runoff volume.
586 *Proceedings of the ICE–Water Management*. **162**(5), 329–336.

587 Kjeldsen, T. R. & Jones, D. A. 2009 A formal statistical model for pooled analysis of
588 extreme floods. *Hydrol. Res*. **40**(5), 465–480.

589 Kjeldsen, T. R. & Prosdocimi, I. 2015 A bivariate extension of the Hosking and Wallis
590 goodness-of-fit measure for regional distributions. *Water Resour. Res.* **51**, 896–907.

591 Klein, B., Pahlow, M., Hundecha, Y. & Schumann, A. 2010. Probability analysis of
592 hydrological loads for the design of flood control systems using copulas. *J. Hydrol.*
593 *Eng*. **15** (5), 360–369.

594 Mediero, L., Kjeldsen, T.R, Macdonald, N., Kohnova, S., Merz, B., Vorogushyn, S.,
595 Wilson, D., Alburquerque, T., Bloeschl, G., Bogdanowicz, E., Castellarin, A., Hall,
596 J., Kobold, M., Kriauciuniene, J., Lang, M., Madsen, H., Onusluel Gul, G, Perdigao,
597 R.A.P., Roald, L.A., Salinas, J.L., Toumazis, A.D., Veijalainen, N. & Odinn
598 Porarinsson. 2015. Identification of coherent flood regions across Europe by using
599 the longest streamflow records. *J. Hydrol*, **528**, 341–360.

600 Mediero, L., Santillán, D., Garrote, L. & Granados, A. 2014 Detection and attribution of
601 trends in magnitude, frequency and timing of floods in Spain. *J. Hydrol*. **517**, 1072–
602 1088.

603 Miller, J. D. & Grebby, S. 2014 Mapping long-term temporal change in imperviousness
604 using topographic maps. *Int. J. Appl. Earth Obs*. **30**, 9–20.

605 Miller, J. D., Kim, H., Kjeldsen, T. R., Packman, J., Grebby, S., & Dearden, R. 2014
606 Assessing the impact of urbanization on storm runoff in a peri-urban catchment
607 using historical change in impervious cover. *J. Hydrol*. **51**(5) 59–70.

608 Petrow, T. & Merz, B. 2009 Trends in flood magnitude, frequency and seasonality in
609 Germany in the period 1951–2002. *J. Hydrol*. **371**, 129–141.

610 Poulin, A., Huard, D., Favre, A.C. & Pugin, S. 2007 Importance of tail dependence in
611 bivariate frequency analysis. *J. Hydrol. Eng.* **12**(4), 394–403.

612 Prosdocimi, I., Kjeldsen, T. R. & Svensson, C. 2014 Non-stationarity in annual and
613 seasonal series of peak flow and precipitation in the UK. *Nat. Hazard. Earth Sys*.
614 **14**, 1125–1144.

615 Prosdocimi, I., Kjeldsen, T. R. & Miller, J. D. 2015 Detection and attribution of
616 urbanization effect on flood extremes using nonstationary flood-frequency models.
617 *Water Resour. Res*. **51**, 4244–4262.

618 Renard, B. & Lang, M. 2007 Use of a Gaussian copula for multivariate extreme value
619 analysis: some case studies in hydrology. *Adv. Water Resour*. **30**, 897–912.

620 Requena, A., Mediero, L. & Garrote, L. 2013 A bivariate return period based on copulas
621 for hydrologic dam design: accounting for reservoir routing in risk estimation.
622 *Hydrol. Earth Syst. Sc.* **17**, 3023–3038.

623 Requena, A. I., Flores, I., Mediero, L. & Garrote, L. 2015 Extension of observed flood
624 series by combining a distributed hydro-meteorological model and a copula-based
625 model. *Stoch. Env. Res. Risk. A*. DOI: 10.1007/s00477-015-1138-x.

626 Rose, S., & Peters, N. E. 2001 Effects of urbanization on streamflow in the Atlanta area
627 (Georgia, USA): a comparative hydrological approach. *Hydrol. Process*. **15**(8),
628 1441–1457.

629 Salvadori, G. & De Michele, C. 2004 Frequency analysis via copulas: Theoretical
630 aspects and applications to hydrological events. *Water Resour. Res*. **40**(12),
631 W12511.

632 Schneider, G., Chicken, E. & Becvarik, R. 2015 *NSM3: Functions and datasets to*
633 *accompany Hollander, Wolfe and Chicken*. Nonparameteric Statistical Methods,
634 Third Edition. R package version 1.3. http://CRAN.R-project.org/package=NSM3.

635 Shastri, H., Paul, S., Ghosh, S. & Karmakar, S. 2015 Impacts of urbanisation on Indian
636 summer monsoon rainfall extremes. *J. Geophys. Res. Atmos*. **120**, 495-516.

637 Sheng, J. & Wilson, J.P. 2009 Watershed urbanization and changing flood behavior
638 across the Los Angeles metropolitan region. *Nat. Hazards*. **48**, 41–57.

639 Shiau, J., Wang, H. & Tsai, C. 2006 Bivariate frequency analysis of floods using
640 copulas. *J. Am. Water Resour. As*. **42**(6), 1549–1564.

641 Shuster, W.D, Bonta, J., Thurston, H., Warnemuende, E. & Smith, D.R. 2005 Impacts
642 of impervious surface on watershed hydrology: a review. *Urban Water J*. **2**(4), 263–
643 275.

644 Sklar, A. 1959 Fonctions de répartition à n dimensions et leurs marges. *Publ. Inst.*
645 *Statist. Univ. Paris*, 8, 229–231.

646 Sraj, M., Bezak, N. & Brilly, M. 2015 Bivariate flood frequency análisis using the
647 copula function: a case study of the Litija station on the Sava River. *Hydrological*
648 *Processes*. **29**, 225–238.

649 Stedinger, J. R. & Griffis, V. W. 2011 Getting from here to where? flood frequency
650 analysis and climate. *J. Am. Water Resour. As*. **47**(3), 506–513.

651 Stedinger, J. & Lu, L. 1995 Appraisal of regional and index flood quantile estimators.
652 *Stoch. Hydrol. Hydraul*. **9**, 49–75.

653 Stedinger, J., Vogel, R. & Foufoula-Georgiou, E. 1993 *Frequency analysis of extreme*
654 *events, Handbook of Hydrology*, Maidment DR, McGraw-Hill Book Company, New
655 York.

656 Villarini, G., Serinaldi, F., Smith, J. A., & Krajewski, W. F. 2009 On the stationarity of
657 annual flood peaks in the continental united states during the 20th century. *Water*
658 *Resour. Res*. **45**(8), W08417.

659 Wilson, D., Hisdal, H. & Lawrence, D. 2010 Has streamflow changed in the Nordic
660 countries?–recent trends and comparisons to hydrological projections. *J. Hydrol*.
661 **394**(3), 334–346.

662 Yue, S., Ouarda, T.B.M.J., Bobée, B., Legendre, P. & Bruneau, P. 1999 The Gumbel
663 mixed model for flood frequency analysis. *J. Hydrol*. **226**, 88–100.

664 Zhang, L. & Singh, V. 2006 Bivariate flood frequency analysis using the copula
665 method. *J. Hydrol. Eng.* **11**(2), 150–164.

Table 1 Summary of the catchment descriptors for the two catchments under study.

Descriptors	Catchment					
	70005 (urban)			72014 (rural)		
AREA[km^2]	54.5			28.99		
BFIHOST	0.473			0.443		
FARL	0.964			0.975		
FPEXT[%]	0.14			0.08		
SAAR[mm]	1021			1183		
Statistics	Season			Season		
	Winter	Summer	Annual	Winter	Summer	Annual
Mean *Q*	22.18	17.31	23.62	16.06	11.42	17.43
Median *Q*	22.78	15.85	22.95	13.85	9.64	16.45
25th quantile *Q*	18.03	9.73	19.78	11.78	8.02	12.95
75th quantile *Q*	24.75	22.18	25.97	21.98	15.45	22.65
Mean *V*	0.57	0.32	0.56	0.28	0.14	0.28
Median *V*	0.50	0.22	0.50	0.26	0.13	0.24
25th quantile *V*	0.40	0.15	0.38	0.16	0.08	0.17
75th quantile *V*	0.63	0.47	0.66	0.38	0.20	0.34

Table 2 Results of the Mann-Kendall test. Values in bold indicate statistically significant trends.

Catchment	Season	Variable	τ	$p-$value
70005	Winter	Q	0.230	0.067
		V	0.097	0.446
	Summer	Q	0.300	**0.016**
		V	0.222	0.077
	Annual	Q	0.276	**0.027**
		V	0.101	0.427
72014	Winter	Q	0.190	0.131
		V	0.214	0.089
	Summer	Q	0.173	0.168
		V	0.133	0.292
	Annual	Q	0.157	0.212
		V	0.099	0.436

Table 3 *P*-values of the trend significance assessment performed by the permutation procedure. Values in bold indicate statistically significant trends.

Catchment	Season	Differences in		
		m_Q	m_V	τ
70005	Winter	0.264	0.644	0.123
	Summer	**0.002**	0.317	0.961
	Annual	0.150	0.362	0.132
72014	Winter	0.213	0.262	0.393
	Summer	0.332	0.256	0.355
	Annual	0.262	0.450	0.465

Table 4 $\hat{\xi}$, $\hat{\sigma}$ and $\hat{\gamma}$ parameters of the marginal distributions of *Q* and *V* (related to annual maximum flow series) fitted by L-moments with a given $\hat{\gamma}$ estimated with the entire data length.

Catchment	Variable	Distribution	Period	Estimated margin parameters		
				$\hat{\xi}$	$\hat{\sigma}$	$\hat{\gamma}$
70005	*Q*	GLO	1976–1992 (W1)	21.679	3.774	-0.162
			1993–2008 (W2)	23.824	2.576	
			1976–2008 (whole series)	22.739	3.222	
	V	GLO	1976–1992 (W1)	0.493	0.154	-0.265
			1993–2008 (W2)	0.497	0.141	
			1976–2008 (whole series)	0.496	0.146	
72014	*Q*	GLO	1976–1992 (W1)	15.717	3.349	-0.079
			1993–2008 (W2)	18.187	3.950	
			1976–2008 (whole series)	16.949	3.675	
	V	GEV	1976–1992 (W1)	0.186	0.103	-0.122
			1993–2008 (W2)	0.214	0.114	
			1976–2008 (whole series)	0.201	0.107	

Table 5 Estimates of the copula parameter and results of the goodness-of-fit test, upper tail dependence measure and AIC for copula selection. Values in bold indicate copulas that pass the test.

Catchment	Time period	Copula	$\hat{\theta}$	S_n	*p*-value	$\hat{\lambda}_U^{CFG}$	$\hat{\lambda}_U$	AIC
70005	1976–1992 (W1)	Clayton	2.286	0.055	**0.126**	0.604	0	-5.719
		Frank	6.377	0.043	**0.454**		0	-8.870
		Gumbel	2.143	0.046	**0.310**		0.618	-8.036
		Galambos	1.429	0.046	**0.299**		0.616	-8.330
		Plackett	13.869	0.044	**0.403**		0	-8.009
	1993–2008 (W2)	Clayton	7.231	0.049	**0.066**	0.803	0	-3.634
		Frank	16.636	0.035	**0.439**		0	-25.318
		Gumbel	4.615	0.036	**0.341**		0.838	-20.228
		Galambos	3.906	0.036	**0.345**		0.837	-19.892
		Plackett	95.667	0.037	**0.354**		0	-22.482
	1976–2008 (whole series)	Clayton	3.043	0.060	0.004	0.664	0	-2.391
		Frank	8.022	0.034	**0.219**		0	-27.034
		Gumbel	2.522	0.031	**0.244**		0.684	-26.040
		Galambos	1.810	0.031	**0.241**		0.682	-26.101
		Plackett	21.622	0.034	**0.196**		0	-25.201
72014	1976–1992 (W1)	Clayton	3.371	0.039	**0.544**	0.686	0	-16.647
		Frank	8.717	0.032	**0.868**		0	-13.654
		Gumbel	2.685	0.031	**0.899**		0.706	-12.614
		Galambos	1.974	0.031	**0.903**		0.704	-12.794
		Plackett	25.516	0.032	**0.889**		0	-12.932
	1993–2008 (W2)	Clayton	1.705	0.080	0.009	0.555	0	-5.572
		Frank	5.057	0.063	**0.069**		0	-5.036
		Gumbel	1.853	0.056	**0.116**		0.546	-5.055
		Galambos	1.136	0.056	**0.123**		0.543	-4.796
		Plackett	9.102	0.062	**0.081**		0	-5.400
	1976–2008 (whole series)	Clayton	2.062	0.060	0.010	0.575	0	-20.427
		Frank	5.876	0.041	**0.113**		0	-17.136
		Gumbel	2.031	0.033	**0.249**		0.593	-15.451

	Galambos	1.316	0.033	**0.244**	0.591	-14.958
	Plackett	11.908	0.038	**0.142**	0	-18.086

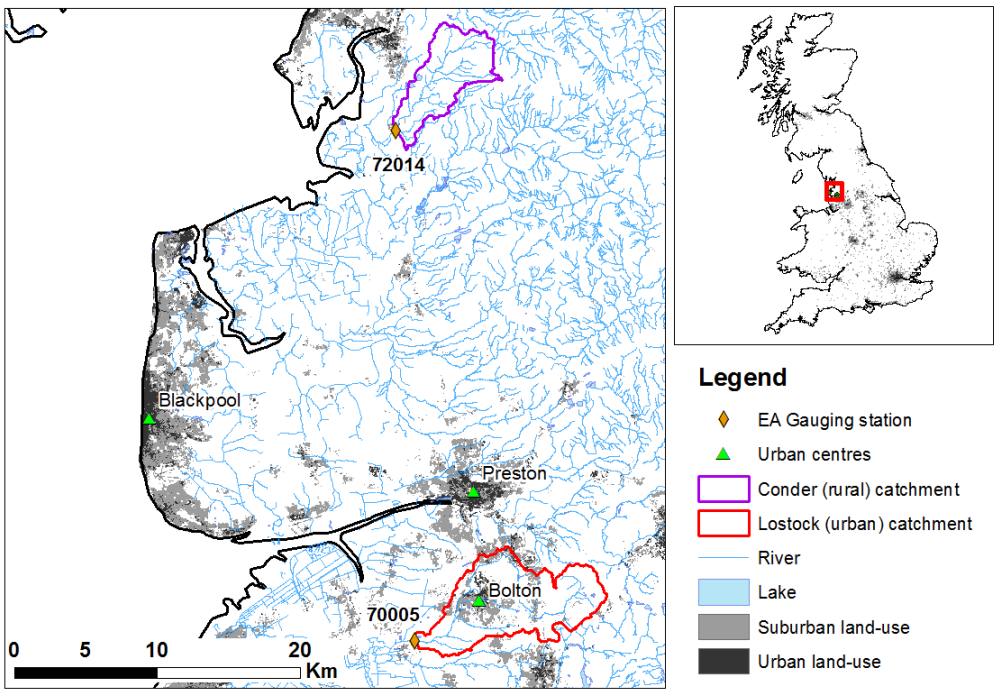

Figure 1 Location of the catchments.

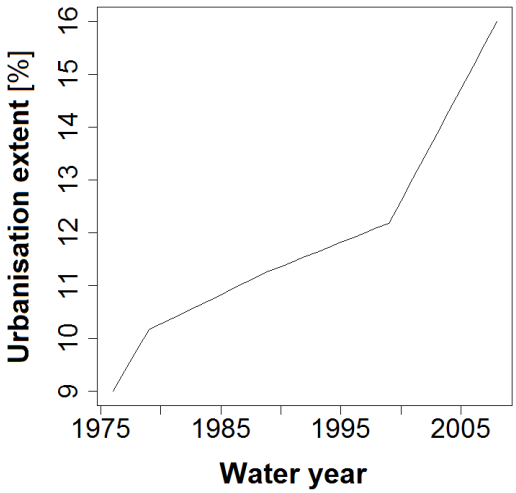

Figure 2 Evolution in time of the urbanisation level of Catchment 70005.

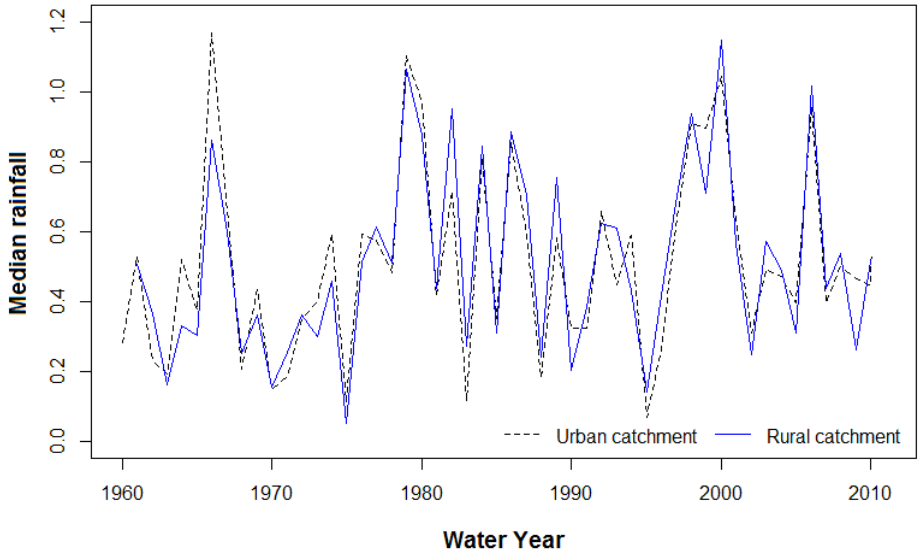

Figure 3 Example: median average daily rainfall series of the urban and rural catchments.

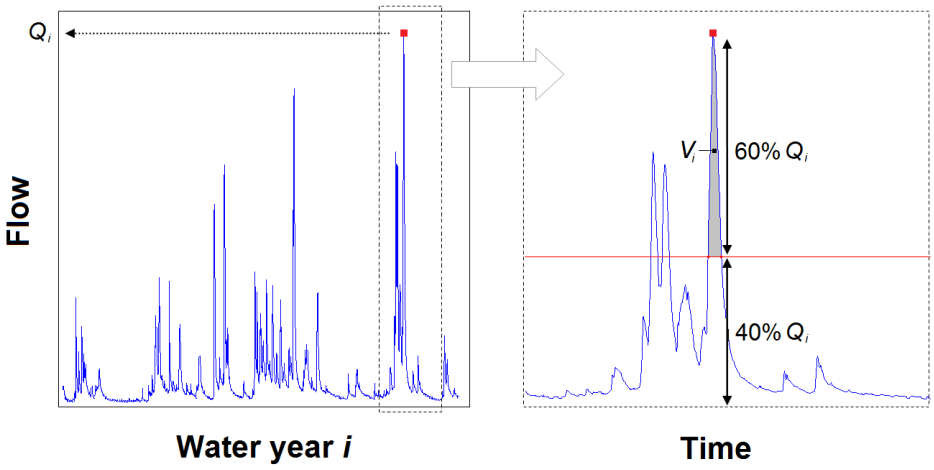

Figure 4 Example of (Q_i, V_i) extraction from a given water year *i*.

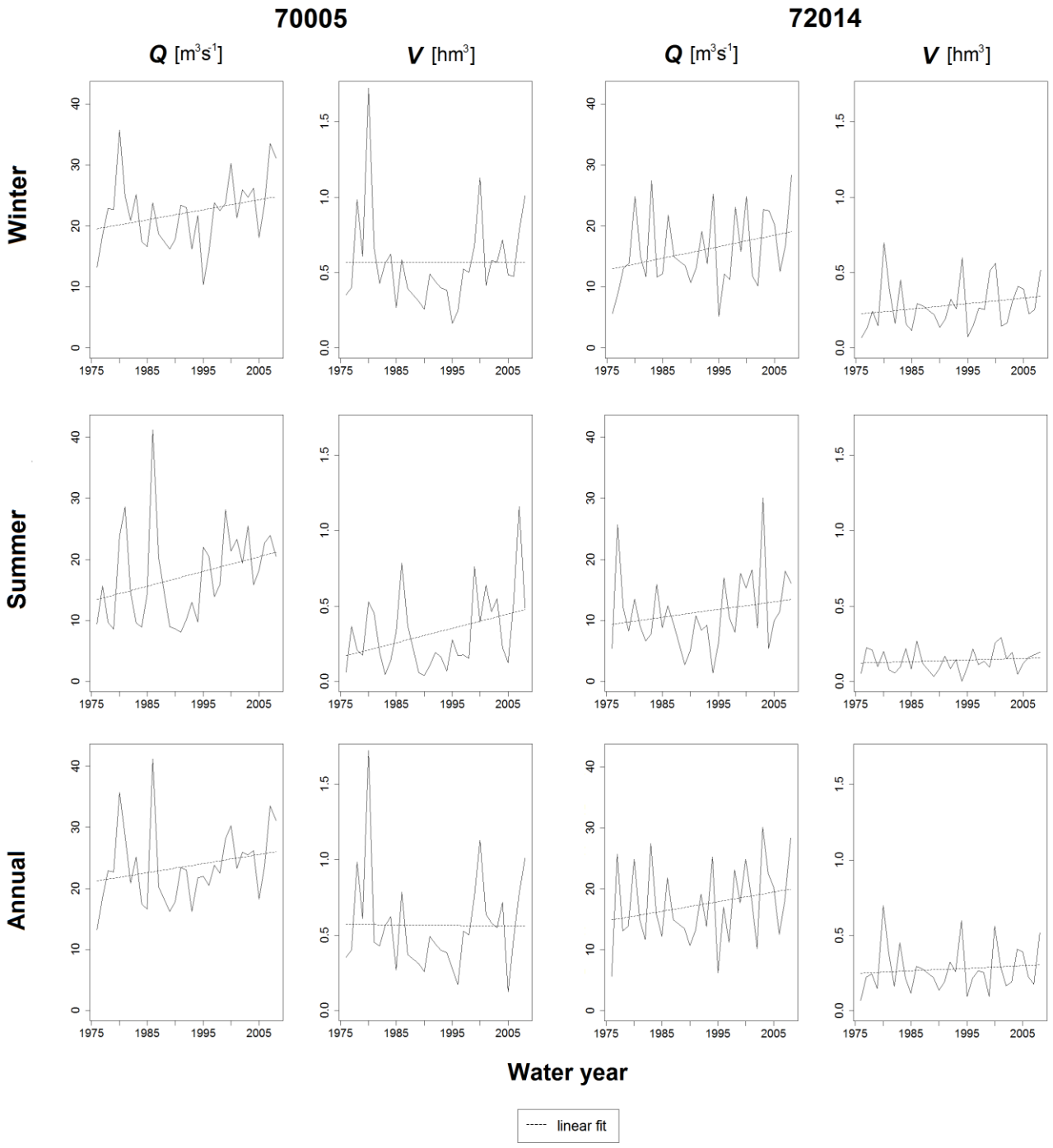

Figure 5 Evolution in time of *Q* and *V*.

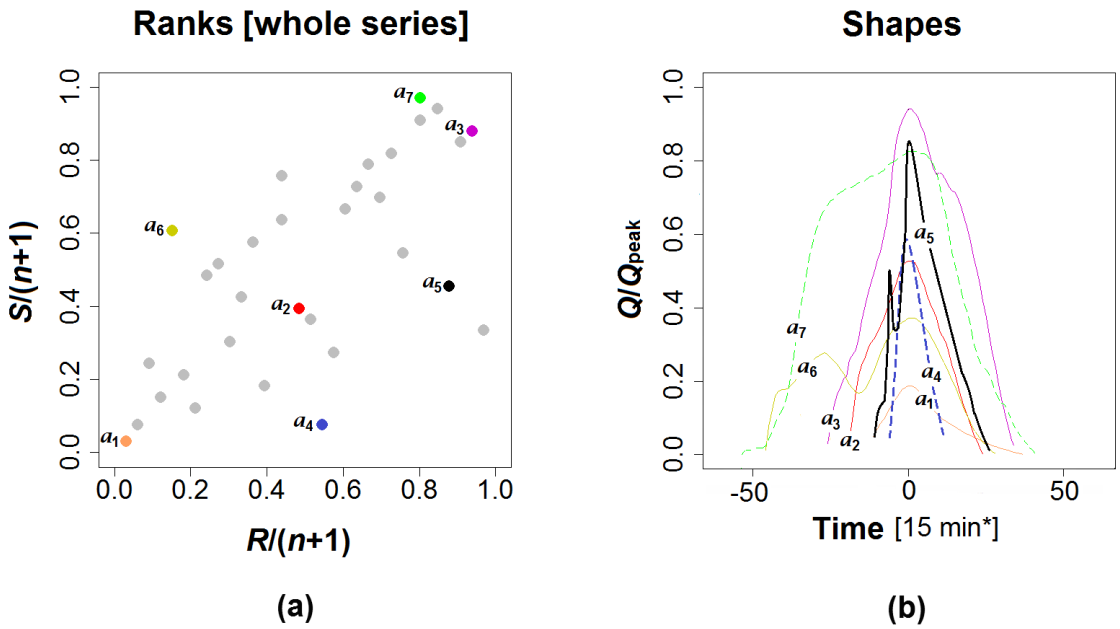

Figure 6 Example of hydrograph shapes corresponding to different pairs of ranks: a) ranks; b) hydrograph shapes.

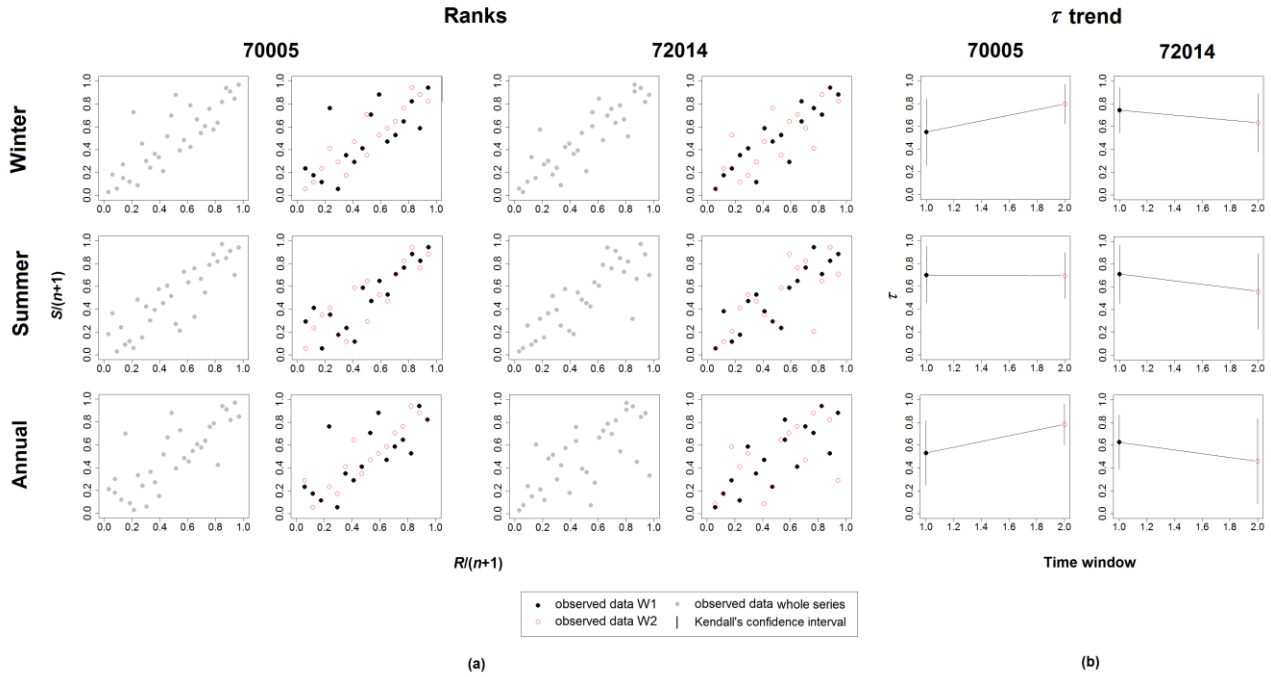

Figure 7 Ranks considering (by columns): a) whole data length, and data belonging to W1 and W2. b) Kendall's τ trend obtained from the two time windows.

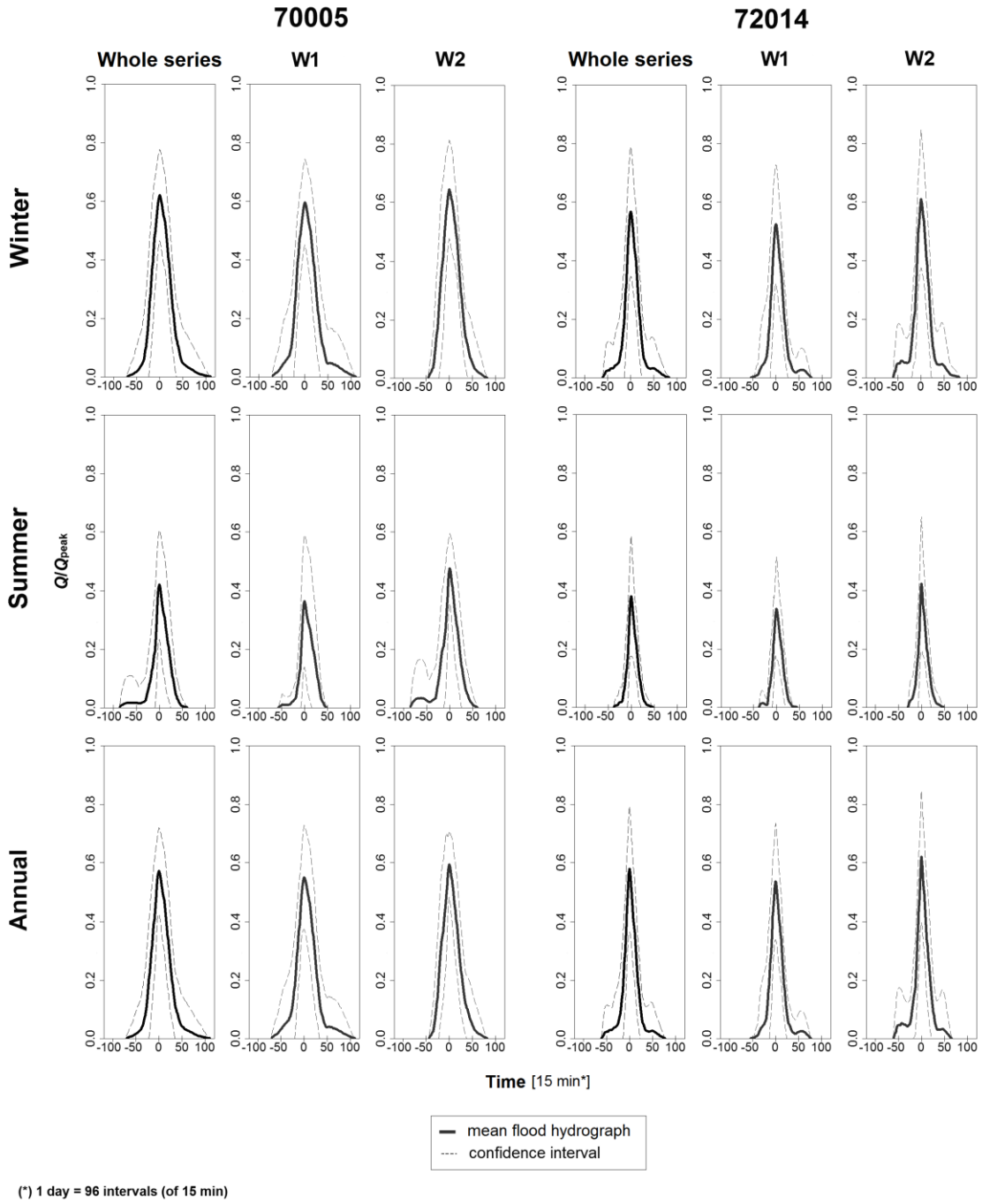

Figure 8 Mean and confidence interval of the hydrograph shape.

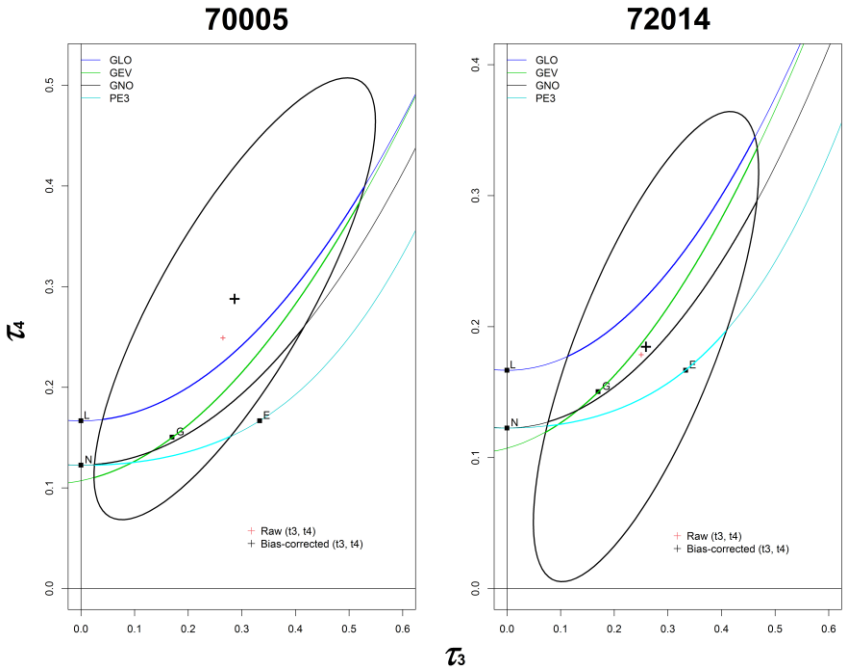

Figure 9 L-moment ratio diagram for the complete *V* series. The 95% ellipse identifying the acceptable distribution according to the Kjeldsen and Prosdocimi (2015) measure are also shown.

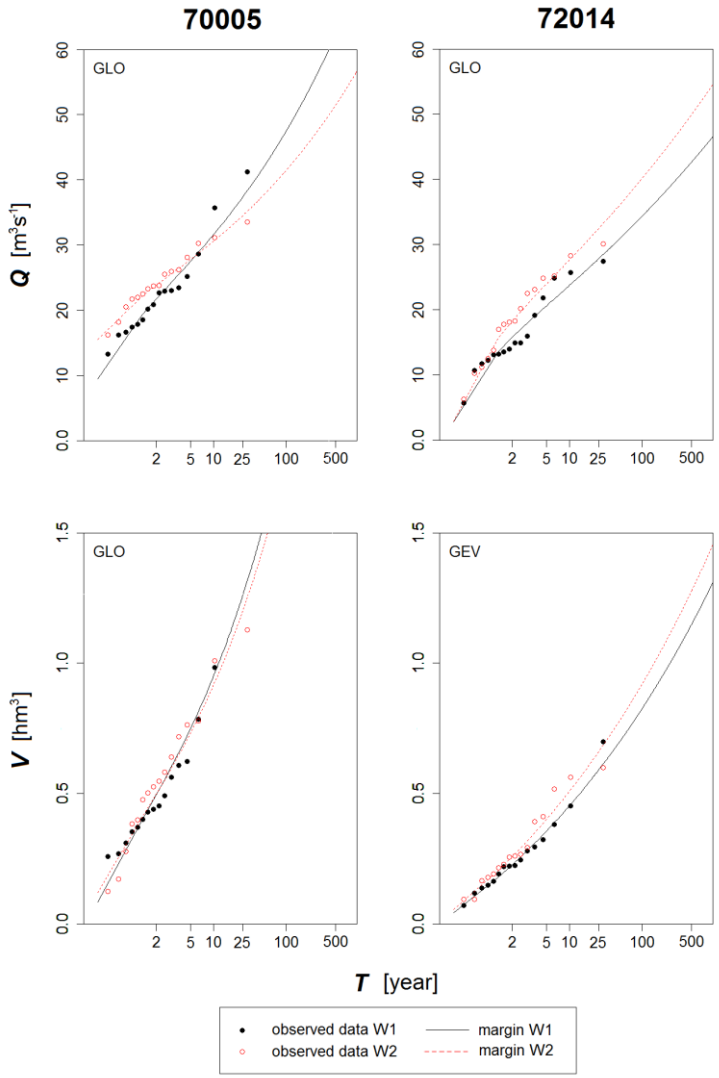

Figure 10 Fit of the selected marginal distribution (of annual maximum flow events) to the observed data for the two time windows.

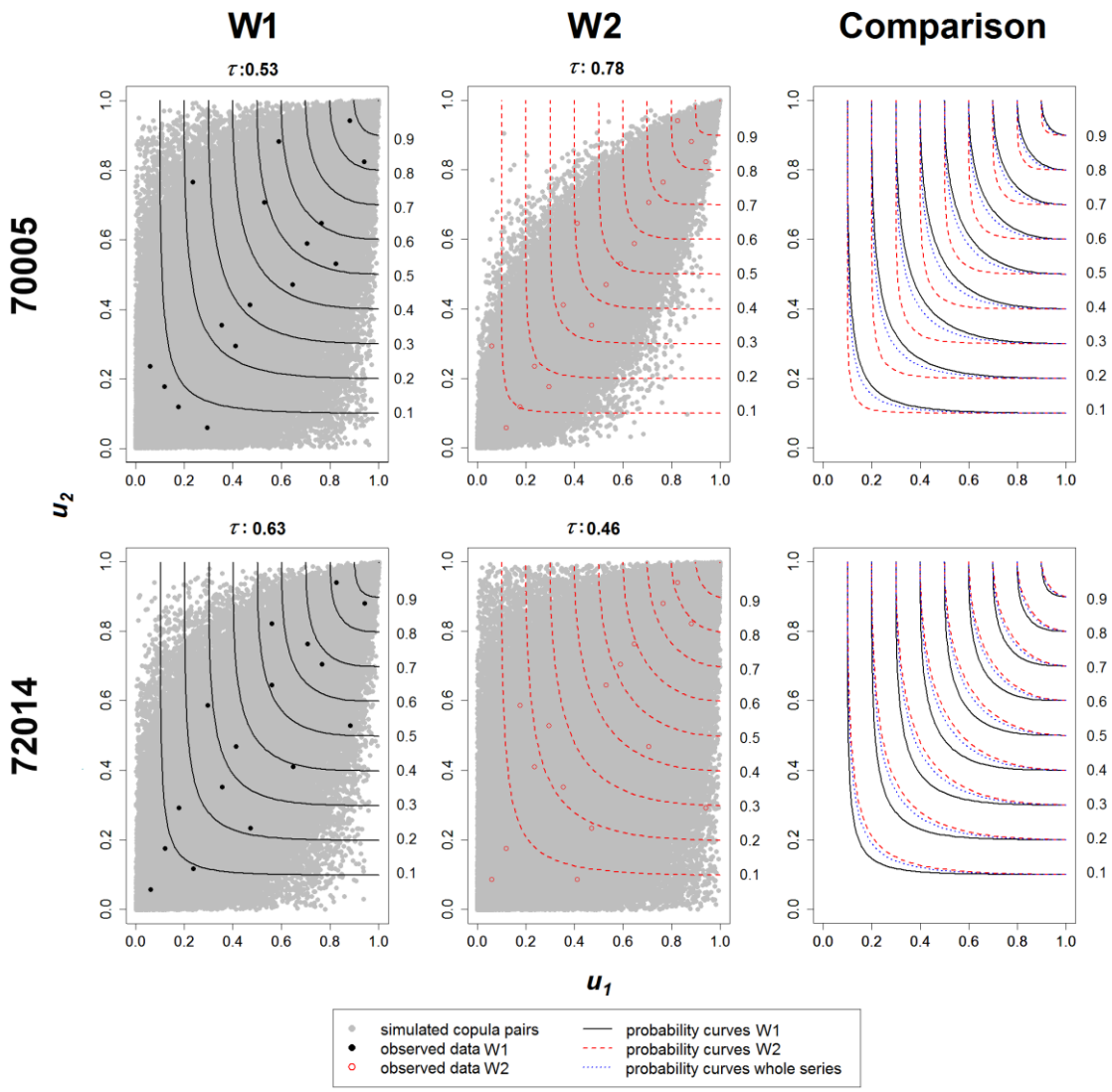

Figure 11 Probability level curves, and observed and simulated (u_1, u_2) data (copula scale) for time periods W1, W2 and whole data length.

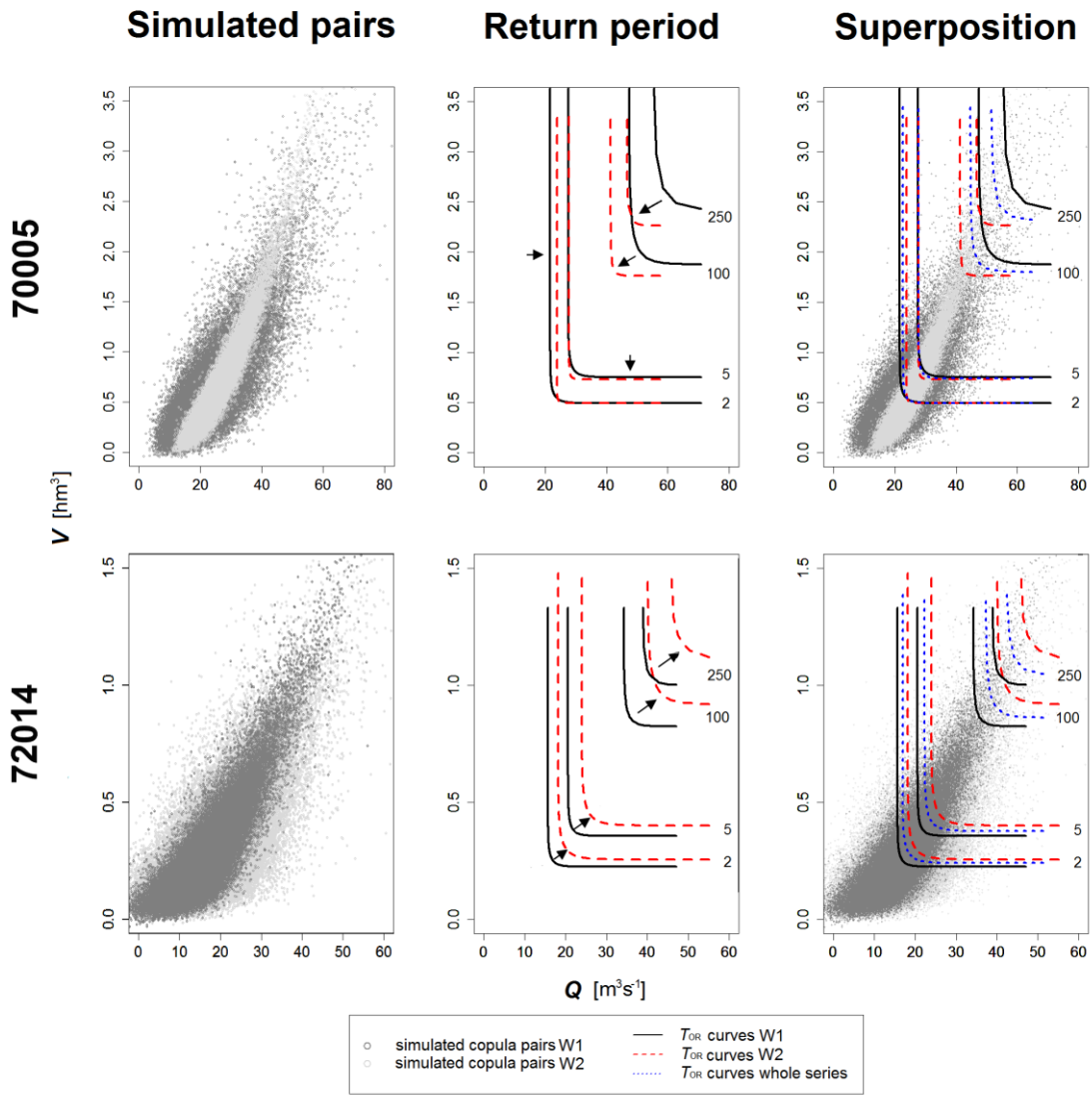

Figure 12 Simulated data and comparison among return period curves (original units) for W1, W2 and whole data length.